



Smart elasto-magneto-electric (EME) sensors for stress monitoring of steel structures in railway infrastructures^{*}

Yuan-feng DUAN^{†1}, Ru ZHANG¹, Yang ZHAO^{†‡1}, Siu-wing OR², Ke-qing FAN³, Zhi-feng TANG¹

⁽¹⁾College of Civil Engineering and Architecture, Zhejiang University, Hangzhou 310058, China

⁽²⁾Department of Electrical Engineering, The Hong Kong Polytechnic University, Hong Kong, China

⁽³⁾School of Information Engineering, Wuyi University, Jiangmen 529020, China

[†]E-mail: cezyduan@zju.edu.cn; ceyzhao@zju.edu.cn

Received Sept. 23, 2011; Revision accepted Sept. 23, 2011; Crosschecked Sept. 26, 2011

Abstract: Steel structures are widely used in railway infrastructures. Their stress state is the most important determinant of the safety of these structures. The elasto-magnetic (EM) sensor is the most promising for stress monitoring of in-service steel structures. Nevertheless, the necessity of magnetic excitation to saturation due to the use of a secondary coil for signal detection, keeps from its engineering application. In this paper, a smart elasto-magneto-electric (EME) sensor using magneto-electric (ME) sensing units to take the place of the secondary coil has been exploited for the first time. The ME sensing unit is made of ME laminated composites, which has an ultrahigh ME voltage coefficient and can measure the magnetic induction simply and precisely. Theoretical analysis and characterization experiments firstly conducted on the ME laminated composites showed that the ME sensing units can be applied in the EM sensor for improved performance in stress monitoring. A tension test of a steel bar was carried out to characterize our smart EME sensor and the results showed high accuracy and sensitivity. The present smart EME sensor is a promising tool for stress monitoring of steel structures in railway and other civil infrastructures.

Key words: Stress monitoring, High-speed railway, Steel rail, Elasto-magnetic (EM) sensor, Magneto-electric (ME), Elasto-magneto-electric (EME) sensor

doi:10.1631/jzus.A11GT007

Document code: A

CLC number: U216.42⁺⁴

1 Introduction

Steel structures are widely used in railway infrastructures, such as roofs of railway stations, large span cable-stayed bridges, suspension bridges, and steel rails. Structures and facilities under long-term dynamic/static loads deteriorate over time and may become unsafe. Monitoring their stress state is crucial for safety evaluation and in deciding whether to pro-

long their service life or to retrofit them. The fracture of critical steel components may induce the failure of whole roofs. Damage to steel cables may result in the collapse of whole bridges. The stress distribution in steel rails has a significant influence on the growth rate of cracks and thus affects the occurrence of rail failures (Cannon and Pradier, 1996; Sasaki *et al.*, 2008). The stress state of steel rails is the most important determinant for the proper maintenance and for failure prevention of railways, especially for high-speed railways (Cannon *et al.*, 2003; Ekberg and Kabo, 2005). However, the non-destructive stress monitoring of in-service steel structures is still a challenging task for civil engineering communities. The current stress monitoring methods, such as those using electric resistance-, vibrating wire-, or optical fiber-strain gauges, or the vibrating frequency

[‡] Corresponding author

^{*} Project supported by the National Natural Science Foundation of China (Nos. 50908202, 51178426, 90915008, and 60801011), the Zhejiang Provincial Natural Science Foundation, China (No. Y1090382), the Fok Ying-Tong Education Foundation for Young Teachers in the Higher Education Institutions of China (No. 122012), and the Key Science and Technology Innovation Team Program of Zhejiang Province, China (No. 2010R50034)

© Zhejiang University and Springer-Verlag Berlin Heidelberg 2011

method, are unable or unable easily to measure the actual stress (not the relative variation of stress) of in-service steel structures.

An elasto-magnetic (EM) sensor is a promising tool for stress monitoring of steel structures, due to its outstanding superiorities including corrosion resistance, actual-stress measurement, nondestructive monitoring, and long service life. It is composed of a primary coil providing variable flux to the measured steel component, and a secondary (sensing) coil picking up the induced electromotive force that is directly proportional to the change rate of the applied magnetic flux according to Faraday's law of electromagnetic induction. In recent years, several investigators (Kvasnica and Fabo, 1996; Wang *et al.*, 1998; 2001; Wang and Wang, 2004; Tang *et al.*, 2008) have developed magnetoelastic theory-based systems that are being applied to monitor the stress of civil engineering structures. Kvasnica and Fabo (1996) developed a microcomputer-based instrument as an application of magnetoelastic theory for the investigation of new principles in the non-destructive measurement of large mechanical stress. They found that the change of permeability with tension was linear during the magnetic saturation of the low-carbon steel wires used in the building industry. Wang *et al.* (1998) introduced the concept of utilizing a novel sensor technology for monitoring structures. They also developed, fabricated, and tested an EM sensor for the direct measurement of stress in steel cables. The sensor was magnetized by a removable C-shaped circuit, rather than by a solenoid (Wang *et al.*, 2001). They later exploited a U-shaped EM sensor (Wang and Wang, 2004). Tang *et al.* (2008) devised a steel strand tension sensor with a different single bypass excitation structure to solve the temperature and installation problems. These techniques, in addition to conventional stress monitoring techniques (Sasada *et al.*, 1986; Seekircher and Hoffmann, 1989; Kleinke and Uras, 1994; Bartels *et al.*, 1996; Brophy and Brett, 1996), are continuously increasing our ability to monitor stress and damage in real time and to obtain an accurate assessment of the actual and future performance of a structure.

Nevertheless, some problems restrict the application of such EM sensors. To magnetize the steel

members to magnetic saturation, the primary coil usually has to be large. Precise installation of the secondary coil in accordance with theoretical assumptions and principles is not easy and normally requires skilled technique and a coiling machine. The use of a secondary coil as the signal detection element requires signal integration, which takes a long time and results in a non-real-time monitoring mode. Furthermore, the coils themselves influence the signals due to interference and noise components, resulting in lower accuracy.

This paper presents a novel smart elasto-magneto-electric (EME) sensor for stress monitoring of steel structures, in which the secondary coil is replaced by magneto-electric (ME) laminated composites as the sensing unit. A steel bar was selected as a test specimen. After introducing its working principles, we describe the testing and verification of the performance of the ME sensing unit using a Hall device. A tension test of the selected steel bar was carried out to characterize the developed smart EME sensor.

2 Tested steel bars

Cylindrical bars, 12 mm in diameter and 800 mm in length, made of steel 45 and processed according to the Chinese National Standard "Quality Carbon Structural Steels" (GB/T699-1999) were used in this study. Their chemical composition and mechanical properties are presented in Tables 1 and 2, respectively. The magnetic properties of this material can be described as follows: coercivity H_c is 592 A/m, remanence B_r is 0.9 T, maximum relative permeability μ_{rm} is 583 and the corresponding magnetic field strength H is 960 A/m, and the maximum magnetic energy product $(HB)_{max}$ is 0.2 kJ/m³. These data served as a reference to test the reliability of our experiments. The magnetic characteristic curves (Bozorth, 1951; Ke *et al.*, 2003), including the fundamental magnetization curve ($B-H$), the permeability curve ($\mu-H$), the remanence curve (B_r-H), and the hysteresis loop (the descending parts in the first and second quadrants), are shown in Fig. 1 (Bozorth, 1951; Ke *et al.*, 2003). All the tests were conducted at room temperature to avoid thermal fluctuation.

Table 1 Chemical composition of the steel bars

Designation	Unified numerical code	Element (%)					
		C	Si	Mn	Cr	Ni	Cu
45	U20452	0.42–0.50	0.17–0.37	0.50–0.80	≤0.25	≤0.30	≤0.25

Table 2 Mechanical properties of the steel bars

Designation	Tensile strength (MPa)	Yield strength (MPa)	Elongation (%)	Percentage reduction of area (%)	Hardness of steel material in delivery state	
					Non-heat treated steel	Annealed
45	≥600	≥355	≥16	≥40	≤229	≤197

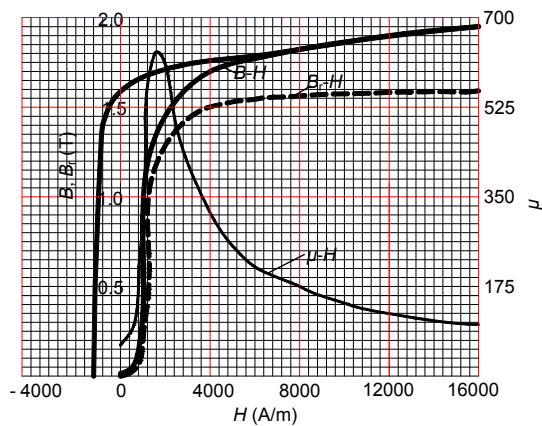


Fig. 1 Magnetic characteristic curves of the tested steel bars

3 Magneto-electric sensing unit

3.1 Working principle

Fig. 2 shows a photograph of the proposed smart sensing unit, which was made of a Terfenol-D alloy/Pb(Zr_{0.52}Ti_{0.48})O₃ (PZT) ceramic ME laminated composite (Jia *et al.*, 2007; Wang *et al.*, 2008a; 2008b). This is a new form of magnetostrictive/piezoelectric composite material with superior ME effect due to the product effect of the piezoelectric effect and the magnetostrictive effect (Dong *et al.*, 2003). The plates were 12 mm long, 6 mm wide, and 1 mm thick. Under the action of an external magnetic field, mechanical strains arise in the sandwiched Terfenol-D plate due to a magnetostriction effect. These strains are transferred to the PZT plate through the adhesive layer, where they produce an electric signal owing to the piezoelectric effect. The magnetic sensor can be used to measure both direct current (DC) and alternating current (AC) magnetic fields

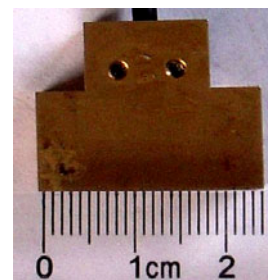


Fig. 2 ME sensing unit

without an external power supply, either in a 1D or multi-dimensional magnetic field, and can produce a large output voltage in real time, 2000 times higher than the traditional Hall devices. The structure and design of the magnetic sensor are very simple, and each sensing unit is a magnetic component made of smart materials in a packaged solid state. Because of its ultrahigh ME voltage coefficients α_v , defined by an induced electrical voltage in response to an applied

AC magnetic field $\left(\frac{dV}{dH}\right)$, this magnetic sensor was adopted as the power-free ME sensing unit in our smart EME sensor. Significant advantages such as convenience, low cost, small size, a large magnetic conversion coefficient, fast response, and high sensitivity make these magnetic/piezoelectric laminated materials suitable for the design of the smart EME sensor.

3.2 Performance tests

In practical applications, for a given ME voltage coefficient α_v and the magnetic induction B_G , the peak-to-peak value of the ME sensing unit output $V_{ME,pp}$ can be obtained:

$$V_{ME,pp} = \alpha_v \cdot B_G \tag{1}$$

Therefore, performance tests of the ME sensing unit were conducted as shown in Fig. 3. The main instruments included an oscilloscope, a signal generator, and a power amplifier.



Fig. 3 Experimental setup for determining the relationship between V_{ME} (mV) and B (mT)

By energizing the solenoid with an AC current supply (YE1311 Series Sweep Signal Generator, SINOCERA Piezotronics, Inc.) and a power amplifier (YE5871 Power Amplifier, SINOCERA Piezotronics, Inc.) at the desired amplitude and frequency, a magnetic field was generated inside the coil. The value of the magnetic induction was reflected by the output of the ME sensing unit V_{ME} .

To calibrate and verify the ME sensing unit, a Hall probe connected to a Gaussmeter (Model 410) was also used to measure the magnetic induction B_G . $V_{ME,pp}$ was obtained from the oscilloscope. From the slope of B_G - $V_{ME,pp}$ plot, α_v was determined. The results of the performance tests of the ME sensing unit are shown in Figs. 4 and 5.

Fig. 4a illustrates the waveforms of the measured output (V_{ME}) of the ME sensing unit due to an applied AC voltage V_{in} with the peak-to-peak value of 40.4 V and the frequency of 120.0 Hz. It is clear that V_{ME} follows V_{in} steadily and has a maximum peak-to-peak amplitude of 211.6 mV. The fact that V_{ME} and V_{in} are in opposite phase can be explained by the negative sign of the piezoelectric coefficient in the expression of α_v (Jia et al., 2007).

Fig. 4b plots $V_{ME,pp}$ and B_G as a function of input peak voltage $V_{in,pp}$ at a frequency of 120.0 Hz. The linear regression equation of $V_{ME,pp}$ and $V_{in,pp}$ is $y_1=10.26x-1.815$, with the correlation coefficient $R=0.998$, and the linear regression equation of B_G and $V_{in,pp}$ is $y_2=0.040x-0.0860$, with the correlation coef-

ficient $R=0.999$, indicating good linearity between $V_{ME,pp}$ and B_G .

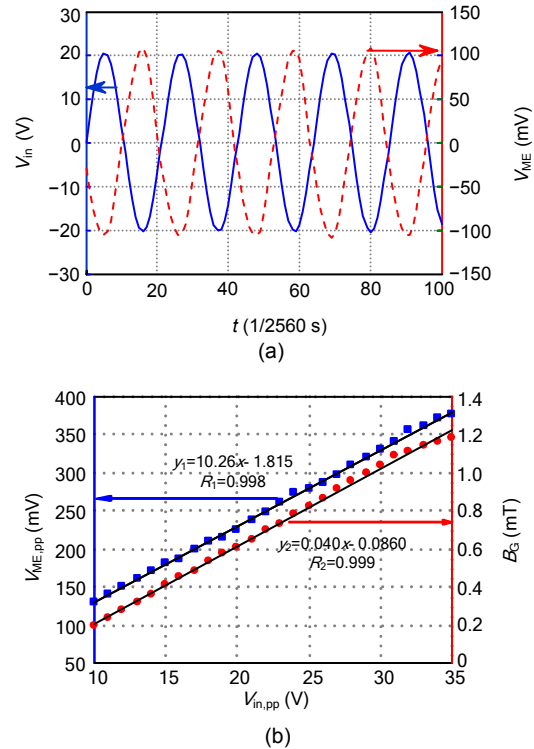


Fig. 4 Measured time-history of V_{ME} due to an applied AC voltage V_{in} (a) and $V_{ME,pp}$ and B_G as a function of $V_{in,pp}$ (b) at the frequency of 120.0 Hz

Fig. 5a shows the relationship between V_{ME} and B_G with the applied AC voltage at the frequency of 120.0 Hz. Its linear regression equation $y=254.6x+20.48$ and correlation coefficient $R=0.997$, which suggests that there is good linearity between the output signals of the smart sensing unit and the magnetic induction B_G , and thus can be used to measure the magnetic induction. Similarly, $V_{ME,pp}$ as a function of the measured B_G and the linear regression equations for some other excitation frequencies are plotted in Fig. 5b. $V_{ME,pp}$ has good linear responses to the magnetic induction in the measured ranges, and α_v at each certain excitation frequency can be determined from the slopes of the B_G - $V_{ME,pp}$ plot.

Note that the ME sensing unit exhibits good linearity for a certain excitation frequency in the range of 100–1000 Hz. To obtain a high and stable conversion factor, this specific range of excitation frequency should be utilized in the design and operation of the sensing unit and its associated devices.

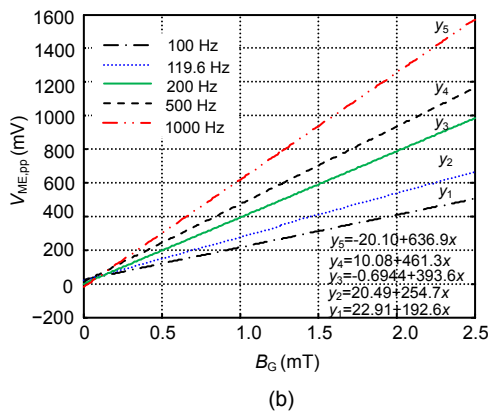
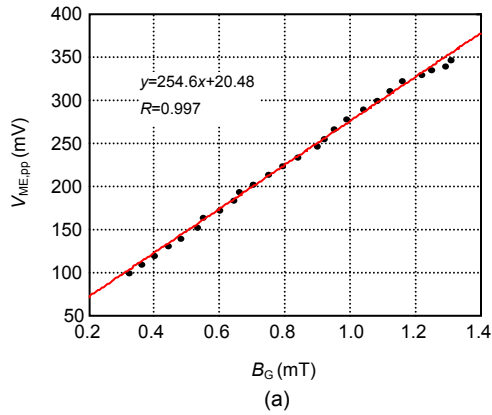


Fig. 5 Relationship between $V_{ME,pp}$ and B_G with the applied AC voltage at the frequency of 120.0 Hz (a) and at various frequencies (b)

4 Smart EME sensor and tension tests

The smart EME sensor is composed of the energizing apparatus providing the necessary magnetic field and the ME sensing unit measuring the magnetic field under various stresses.

The tests were conducted using the setup as shown in Fig. 6. Axial stress below the yield strength was applied through the tension testing machine (CSS5200, SANS), which was operated in accordance with the pre-set procedures, including the loading magnitude and speed. The proportional limit in the stress of this wire is 353 MPa (the limit tension of the tested steel bar is 40 kN). The tests were conducted at room temperature and with the tension in the range of 0 to 20 kN at 2 kN intervals. The peak of input voltage $V_{in,pp}$ was 41.0 V and the frequency was 120.0 Hz. Dynamic signal acquisition and processing in the experiment was performed by the data acquisition card and signal conditioning instruments (Fig. 7).



Fig. 6 Experimental setup for tension tests



Fig. 7 Signal conditioning and data acquisition instruments

The sinusoidal input voltages to the solenoid and the output signals from the sensing unit were recorded by the data acquisition and analysis system. Each data point was obtained by averaging the results of ten tests, with deviation no larger than 1% (Fig. 8). The linear regression equation of $V_{ME,pp}$ and T (tension in kN) was $y_1=217.8+1.042x$, with a correlation coefficient of $R=0.998$, for the loading process. For the unloading process, the linear regression equation of $V_{ME,pp}$ and T was $y_2=216.4+1.108x$, with a correlation coefficient of $R=0.986$. Therefore, a good linearity between $V_{ME,pp}$ and T is indicated. The error was below 1% and the repeatability was good, as observed in the tests.

Several factors may have contributed to the differences between the loading and unloading results including: the existence of residual deformation and initial imperfection, the inconsistent force-displacement curves (Fig. 9), the non-uniformity of the material, and the impact of loading conditions (both ends are clamped) resulting in distortion of the steel bars. So the results for the loading process

should be more reliable and were selected for analysis. The measurement result was in accordance with the theoretical analysis of the sensor. The correlation coefficient of linear regression exceeded 0.99 and the repeating error of the sensor was less than 0.15% (Fig. 10).

5 Conclusions

A novel smart EME sensor has been developed, fabricated, and tested. Compared to conventional coil-wound EM sensors, our smart EME sensor has distinct advantages due to the replacement of the sensing coil by an ME sensing unit. The new EME sensor with an ME sensing unit is small, lightweight, and easy to install. Its high precision and good repeatability are demonstrated by our test results. Thus, it is suitable for stress monitoring, with increased sensitivity in real-time of steel structures in railway and other civil infrastructures, such as the roofs of railway stations, large span cable-stayed bridges and suspension bridges, and steel rails.

References

Bartels, K.A., Kwun, H., Hanley, J.J., 1996. Magnetostrictive sensors for the characterization of corrosion in rebars and prestressing strands. *Proceedings of SPIE*, **2946**:40-50. [doi:10.1117/12.259151]

Bozorth, R.M., 1951. *Ferromagnetism*. IEEE Press, New York, USA.

Brophy, J.W., Brett, C.R., 1996. Guided UT wave inspection of insulated feedwater piping using magnetostrictive sensors. *Proceedings of SPIE*, **2947**:205-209. [doi:10.1117/12.259168]

Cannon, D.F., Pradier, H., 1996. Rail rolling contact fatigue research by the European Rail Research Institute. *Wear*, **191**(1-2):1-13. [doi:10.1016/0043-1648(95)06650-0]

Cannon, D.F., Edell, K.O., Grassie, S.L., Sawley, K., 2003. Rail defects: an overview. *Fatigue and Fracture of Engineering Materials and Structures*, **26**(10):865-886. [doi:10.1046/j.1460-2695.2003.00693.x]

Dong, S.X., Li, J.F., Viehland, D., 2003. Ultrahigh magnetic field sensitivity in laminates of TERFENOL-D and $Pb(Mg_{1/3}Nb_{2/3})O_3-PbTiO_3$ crystals. *Applied Physics Letters*, **83**(11):2265-2267. [doi:10.1063/1.1611276]

Ekberg, A., Kabo, E., 2005. Fatigue of railway wheels and rails under rolling contact and thermal loading—an overview. *Wear*, **258**(7-8):1228-1300. [doi:10.1016/j.wear.2004.03.039]

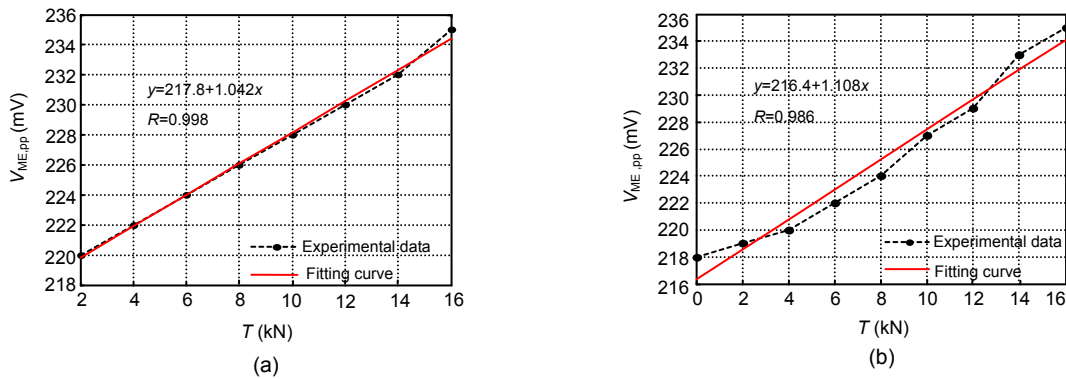


Fig. 8 Relationship between $V_{ME,pp}$ and T under loading (a) and unloading (b) processes

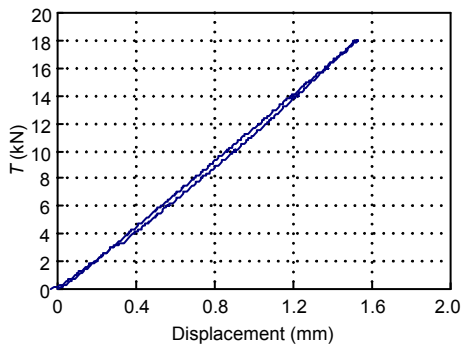


Fig. 9 Force-displacement curve during the loading and unloading processes

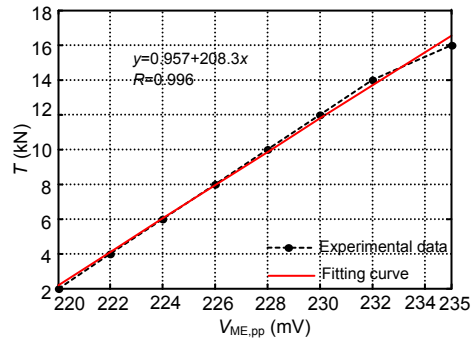


Fig. 10 Measured results of the tension tests

- GB/T 699-1999. Quality Carbon Structural Steels. National Standard of People's Republic of China (in Chinese).
- Jia, Y.M., Or, S.W., Wang, J., Chan, H.L.W., Zhao, X.Y., Luo, H.S., 2007. High magnetoelectric effect in laminated composites of giant magnetostrictive alloy and lead-free piezoelectric ceramic. *Journal of Applied Physics*, **101**(10):104103. [doi:10.1063/1.2732420]
- Ke, S., Ye, D.P., Zhang, G.J., Su, L.G., 2003. Quick Manual for Magnetic Characteristic Curves of Common Steels. China Machine Press, Beijing, China (in Chinese).
- Kleinke, D.K., Uras, H.M., 1994. A magnetostrictive force sensor. *Review of Scientific Instruments*, **65**(5):1699-1710. [doi:10.1063/1.1144863]
- Kvasnica, B., Fabo, P., 1996. Highly precise non-contact instrumentation for magnetic measurement of mechanical stress in low-carbon steel wires. *Measurement Science and Technology*, **7**(5):763-767. [doi:10.1088/0957-0233/7/5/007]
- Sasada, I., Uramoto, S., Harada, K., 1986. Noncontact torque sensors using magnetic heads and a magnetostrictive layer on the shaft surface-application of plasma jet spraying process. *IEEE Transactions on Magnetics*, **22**(5):406-408. [doi:10.1109/TMAG.1986.1064383]
- Sasaki, T., Takahashi, S., Kanematsu, Y., Satoh, Y., Iwafuchi, K., Ishida, M., Morii, Y., 2008. Measurement of residual stresses in rails by neutron diffraction. *Wear*, **265**(9-10):1402-1407. [doi:10.1016/j.wear.2008.04.047]
- Seekircher, J., Hoffmann, B., 1989. New magnetoelastic force sensor using amorphous alloys. *Sensors and Actuators A: Physical*, **22**(1-3):401-405. [doi:10.1016/0924-4247(89)80002-0]
- Tang, D.D., Huang, S.L., Chen, W.M., Jiang, J.S., 2008. Study of a steel strand tension sensor with difference single bypass excitation structure based on the magneto-elastic effect. *Smart Materials and Structures*, **17**(2):025019. [doi:10.1088/0964-1726/17/2/025019]
- Wang, G.D., Wang, M.L., 2004. The utilities of U-shape EM sensor in stress monitoring. *Journal of Structural Engineering and Mechanics*, **17**(3-4):291-302.
- Wang, M.L., Koontz, S., Jarosevic, A., 1998. Monitoring of Cable Forces Using Magneto-Elastic Sensors. Proceedings of 2nd US-China Symposium Workshop on Recent Developments and Future Trends of Computational Mechanics in Structural Engineering, Dalian, China, p.337-349.
- Wang, M.L., Lloyd, G.M., Hovorka, O., 2001. Development of a remote coil magnetoelastic stress sensor for steel cables. *Proceedings of SPIE*, **4337**:122-128. [doi:10.1117/12.435584]
- Wang, Y.J., Or, S.W., Chan, H.L.W., Zhao, X.Y., Luo, H.S., 2008a. Magnetolectric effect from mechanically mediated torsional magnetic force effect in NdFeB magnets and shear piezoelectric effect in $0.7\text{Pb}(\text{Mg}_{1/3}\text{Nb}_{2/3})\text{O}_3$ - 0.3PbTiO_3 single crystal. *Applied Physics Letters*, **92**(12):123510. [doi:10.1063/1.2901162]
- Wang, Y.J., Cheung, K.F., Or, S.W., Chan, H.L.W., Luo, H.S., 2008b. PMN-PT single crystal and Terfenol-D alloy magnetolectric laminated composites for electromagnetic device applications. *Journal of the Ceramic Society of Japan*, **116**(1352):540-544. [doi:10.2109/jcersj2.116.540]